Chapter

1

WHOLE-ORGAN ENGINEERING WITH NATURAL EXTRACELLULAR MATERIALS

Bahoz Sanaan[1*], X. Frank Walboomers[1], and Pamela C. Yelick[2]

[1] Dept. Dentistry, Radboudumc, Nijmegen, The Netherlands
[2] Department of Orthodontics, Division of Craniofacial and Molecular Genetics, Tufts University School of Dental Medicine, Boston, MA, USA

[*]Corresponding author: bahoz.sanaan@student.ru.nl

Contents

1.1. INTRODUCTION

Since 1994, when Cao *et al.* showcased their auricular implant grown on a mouse's back and thereby inspired the field of biomedical research with awe [1,2], whole-organ engineering has been proof-of-concept and a growing interest in the field of regenerative medicine. Whole-organ engineering attempts concentrate on creating fully functional organs *in vivo*. Therefore it is essential to deepen our understanding of the composition of individual tissues, and the interfaces between tissue types. Besides offering a three-dimensional physical structure to house the cells within a given tissue, the extracellular matrix (ECM) also allows for signal transductions that direct the morphogenetic process integrated into the tissue. Cell-surface receptor binding sites found on ECM molecules promote cell proliferation, differentiation, adhesion, migration and survival. Natural ECMs consist of proteins and polysaccharides secreted by cells. Many of these molecules are 'multimodal', providing binding sites for both cell and ECM protein [3]. Comprehensive reports on specific natural ECM molecules and their respective functions have been published [4-8]. ECM in organ systems comprises two major components, which include the basal lamina and the stromal matrix. Although ECM composition of various tissues can be dissimilar, the basal lamina, found bordering epithelial sheets, primarily consists of collagen IV and laminins, while stromal or interstitial matrices include diverse compositions such as fibrillar collagen I or hyaluronic acid [3].

Incorporating natural materials into engineered tissues and organs has many benefits. As described above these natural molecules provide functional cell and ECM adhesion sites. In addition natural ECM molecules offer improved biocompatibility over synthetic alternatives, as well as genetic conservation in terms of use with xenogenic products [8,9]. Over the years, a shift has been notable. Biomaterials have advanced from incorporating inert materials into the body, to creating bioactive and bioresponsive material implantations, in the pursuit of repairing organ functionality or regenerating tissue. The use of natural ECM materials integrates all of these efforts.

The main focus of this chapter is to showcase the developments in whole--organ engineering, which reclaims natural tissue derived materials and natural / synthetic blends in innovative ways (Table 1). In this chapter, we use the tooth as an illustrative example of a developing organ, and discuss current efforts and future applications toward whole-organ tooth engineering using natural ECM molecules.

Table 1. Natural extracellular matrix molecules incorporated into engineered organs and tissues

Natural ECM components	Engineered organ/tissue	Ref.
Collagens	Cartilage	[2,42]
	Blood vessels	[44,48,49,117]
	Nerves	[45,125]
	Ligament	[54]
	Bladder	[55]
	Teeth	[82, 94-97, 133]
	Lymphoids	[121]
Gelatins	Skin	[51,52,136]
	Blood vessels	[44]
	Cartilage	[135]
Hyaluronic acid/hyaluronan	Blood vessels	[42,117]
	Nerves	[125]
Laminin	Peripheral nerves	[43]
Genipin	Skin	[53,136]
	Nerves	[73]
	Cartilage	[135]
Silk/fibroin	Skin	[53]
	Ligament	[54]
	Mineralized osteodentin	[92]
Chitin/chitosan	Cardiac muscle	[66]
	Bone	[67]
Fibrin	Cardiac muscle	[66]
	Blood vessels	[71]
Syndecan-1	Breast	[69]
Perlecan	Lymph vessel	[123]

1.2. THE CURRENT STATE OF THE ART FOR NATURAL SCAFFOLDS

Even though in an early stage, current progresses in engineering whole organs with natural materials include decellularizing cadaveric or animal tissue for scaffold use, electrospinning nanofiber scaffolds or functionalizing environmentally responsive matrices (Diagram 1). Whereas in decellularization the 3D tissue architecture is reused, maintained and

characterized, electrospun fibers and responsive materials attempt to recreate functional niches for cells within a 3D-fabricated environment. These technologies are thoroughly tested along a continuum from prototypical *in vitro* models to human clinical studies. However, significant information can be acquired through the incorporation of natural ECM molecules in all of these efforts as we advance towards engineered whole organs.

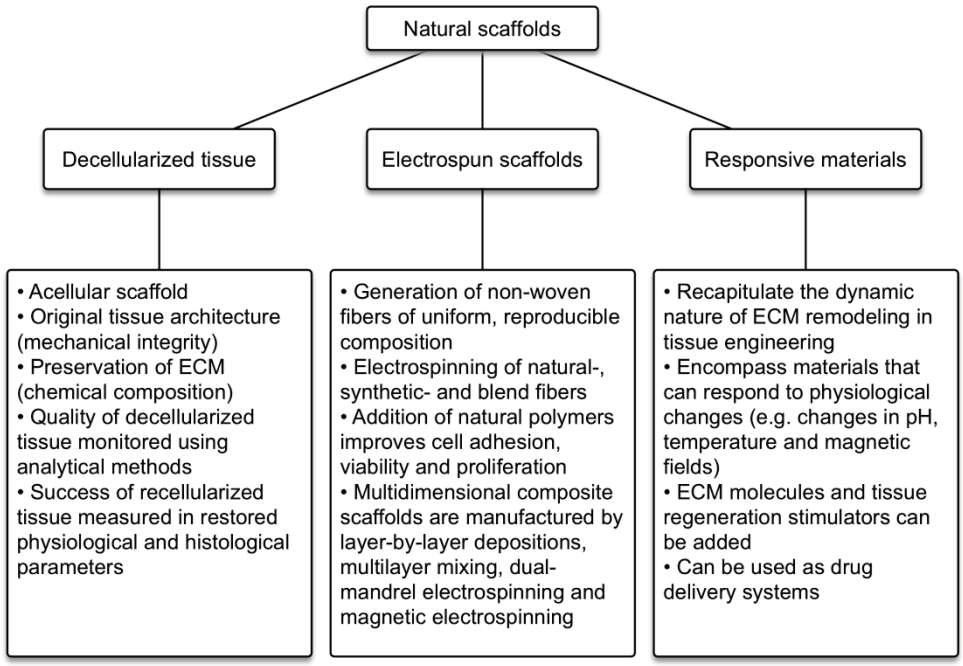

Diagram 1. Schematic diagram summarizing the different natural scaffolds

1.2.1. Decellularization of tissue

Reconstructing a fully functional ECM remains an elusive task. Therefore, decellularization, a gentle process of cell and associated nucleic acid debris removal, has been used to create acellular scaffolds for tissue and organ engineering. These scaffolds retain the original architecture of organs and tissue interfaces, giving rise to a source of allogenic and xenogenic whole--organ grafts. Decellularization has been carried out on a variety of tissues of various organs such as the urinary bladder, small intestinal submucosa, blood vessels, heart valves, pericardium, tooth buds, trachea and esophagus, as well as musculoskeletal regions such as the temporomandibular joint [9-22]. This method of creating acellular scaffolds has resulted in commercial products and tissue substitutes [23-27].

As bioengineering methods advance towards the formation of more complex geometries, the decellularization process has evolved to meet the strict standards needed for allograft studies. As Gilbert *et al.* suggested, there is variability amongst tissue types in terms of effective decellularization methods [24]. While a certain decellularization treatment may efficiently remove cellular material in a given tissues, it may be less effective in another tissue. Denser, thicker tissues and organs may require more robust decellularization methods to insure penetration throughout the tissue, while less dense tissues may require more gentle techniques. In addition, the effectiveness of cell removal and tissue damage varies based upon the method of decellularization (chemical, enzymatic or physical) [13,14,24,28]. Decellularization methods attempting to optimize decellularization reagent incubation time, temperature, concentration or number of solvent cycles, have been reported with varying degrees of success based upon histology, scanning-electron microscopy and mechanical testing of the resulting decellularized scaffold product [12,19,20,28].

In human allograft studies of tracheal tissue, optimized tissue penetration was achieved by circulating cycles of detergents to remove nucleic materials [19,20]. While verification of cell removal is typically quantified by DNA content post-decellularization by means of spectrophotometry [29-32], further characterization of the remaining major histocompatibility complexes (MHCs) is essential for clinical human allograft studies. For the decellularized human whole-trachea graft, MHC class I and II removal was monitored. To decellularize the tissue, multiple washes in 4 % sodium deoxycholate and 2000 kU deoxyribonuclease I were alternated with water rinses. After 25 cycles of detergent washes, immunohistochemistry demonstrated removal of human leukocyte antigen-A (HLA-A), HLA-B and HLA-C antigens, with minimal expression of MHC II antigens. Likewise, serology screens of HLA recipient antidonor antibody production verified complete absence of foreign proteins for as long as 2 months post-surgery [20].

Most of the commonly known decellularization methods require multiple days of treatment, and require large rinsing volumes in order to insure complete decellularization. Novel decellularization procedures based on sodium chloride show promising results in obtaining intact decellularized tissues while significantly reducing the procedure time. Bühler *et al.* have demonstrated the decellularization of full-sized minipig livers within 24 h [33], while Price *et al*. were able to achieve the same using lungs from 20–30 kg pigs using their own method [34]. In both studies collagen and glycosaminoglycans were preserved. However, using these new rapid protocols may require more attention to the preservation of intact ECM components.

Excessive decellularization can degrade the ECM, resulting in collagen damage, glycosaminoglycan depletion, as well as elastin cleavage [24,35]. Accordingly, protocols should be designed to detect and minimize destruction, while preserving the mechanical integrity of the tissue. Often, retention of ECM

architecture is validated in comparison to untreated cadaveric tissue with microscopy to ensure tissue integrity is not compromised [12,13,17,22,28,32,35]. Using histological methods, the extent of ECM damage in collagen-dominated tissue has been quantified by measuring collagen crimping amplitude and periodicity, which can result from exposure to detergents such as sodium dodecyl sulfate [17,35]. Other imaging techniques such as scanning-electron microscopy have been used to visualize and compare nanostructures (*e.g.*, the weave, coil and strut fibers in the decellularized heart study) in decellularized and non-decellularized cadaveric tissue [32]. Together, these studies show that with optimal treatment, decellularized tissues can maintain ECM antibody epitope expression in such molecules as collagens, laminin and fibronectin in immunohistochemistry and immunofluorescence studies [13,15,18,21,30,36]. Table 2 summarizes the various ECM molecules characterized in select decellularized organ and tissue studies.

Just as the chemical composition of the ECM affects organ functionality, mechanical integrity must also be preserved in decellularized tissues. Mechanical testing can be used to quantitatively evaluate the effects of decellularization. As an example, to accommodate ventricular load and associated cardiac stresses, decellularized rat heart cross-sections were demonstrated to exhibit ventricular tissue anisotropy measurements that were similar to cadaveric tissue, with respect to stiffness and tangential modulus.

Table 2. Extracellular matrix molecules characterized in decellularized organ and tissue studies

Natural ECM components	Engineered organ/tissue	Ref.
Collagens	Bladder	[9]
	Blood vessels	[11]
	Heart valve	[12,13,15,17]
	Pericardium	[18]
	Trachea	[20]
	Esophagus	[21]
	Cornea	[28]
	Pulmonary roots	[29]
	Meniscus	[30]
	Ligament	[31,35,36]
	Hearts	[32]
	Teeth	[103]
Laminin	Bladder	[9]
	Heart valve	[13]
	Esophagus	[21]
	Teeth	[103]

Natural ECM components	Engineered organ/tissue	Ref.
Elastin	Blood vessels	[11]
	Heart valve	[12,13,15,17]
	Pericardium	[18]
	Esophagus	[21]
Cytokeratins	Trachea	[4]
Fibronectin	Esophagus	[21]
	Heart	[32]
	Teeth	[103]
Chondroitin sulfate	Meniscus	[30]
Glycosaminoglycans	Bladder	[9]
	Pericardium	[18]
	Heart valve	[12,13,17]
	Meniscus	[30]
	Ligament	[31,35,36]

Recent developments in decellularization methods focus on retaining whole-organ functionality in animal models [32] and in allogenic clinical studies [20]. As mentioned previously, Ott *et al.* has characterized the mechanical properties and ECM composition in an animal model, whereas Macchiarini *et al.* characterized clinical factors for allograft implantation of tracheal tissue in humans. In both studies, decellularization approaches were followed by functional studies of the decellularized tissues, to confirm recapture of the necessary physiologic functions of the recellularized organ.

Measures of restored function have included quantification by physiological parameters. For example, 24 h after recellularization in a coronary perfusion bioreactor, electrical stimulation was introduced in vitro to an entire rat heart. The decellularized rat heart, which was repopulated with a mixed population of cardiac cells, regained approximately 2 % pump function of an adult rat heart, and 25 % pump function of a 16 week fetal human heart as evaluated by its performance under physiologic preload, afterload, intraventricular pressure and electrical stimulation. Furthermore, doses of phenylephrine administered to the recellularized whole heart were also able to stimulate contractility similar to extrinsic control mechanisms that exist physiologically [32]. Likewise, improved muscle contractility force up to 85 % of pre-injury levels was seen after muscle-derived decellularized ECM was implanted in full-thickness defects in the lateral gastrocnemius of Lewis rats. Seven days post-injury, the implanted decellularized ECM were reseeded with bone--marrow-derived mesenchymal stem cells which led to the formation of new muscle tissue [37].

Similarly, in the decellularized human whole-trachea graft study, the restored physiological function of airway clearance in the allogenic, trachea graft was evaluated. The ratio of forced expiratory volume in 1 s to forced vital capacity (FEV1 : FVC) taken before and 3 months after surgery, determined that the graft resulted in a reversal of airway obstruction [20]. As additional clinical studies are completed, we will continue to learn more about the instructive nature of decellularized grafts, including the preservation of angiogenic cytokines [20], as well as other chemokines preserved from previous niches that may affect morphogenesis [4,14,38,39].

1.2.2. Electrospun nanofibers

Electrospinning is a nanofabrication technique that generates nonwoven fibers of uniform, reproducible composition on a physical scale that is topographically compatible with the cells that reside upon them. The ability to electrospin natural materials offers the benefits of incorporated peptide motifs that synthetic materials lack, although natural materials can be too weak to form reproducible nanofibers, and are therefore often blended with biocompatible, synthetic polymers to create composite fibers with added strength [40]. Furthermore, the addition of natural polymers to synthetic fibers has improved the adhesion, viability and proliferation over synthetic material alone [41,42].

Besides having the ability to form nanoscale fibers, 3D assemblies of natural or natural / synthetic blend fibers can also be used to create composite structures, allowing for a closer replication of natural nanoscale ECM fiber composition within an organ. For instance, the basement membrane bordering epithelial sheets consists primarily of fibrillar proteins such as collagen IV and laminin [3]. In terms of structure, electrospun laminin I meshes have recently been fabricated to resemble basement membrane [43]. Bead-like structures, usually indicative of spinning limitations in terms of thinness, were preserved in the laminin spun fibers due to the replication of 'matrisome' structures found in the natural basement membrane. Laminin meshes, in comparison to laminin films, induced more adherent, elongated morphologies commonly associated with neuronal-like cells, as well as β3 tubulin expression in serum-free media, without the use of chemical additives. The addition of exogenous nerve growth factor (NGF) did not increase the frequency of neurite extensions *per* cell, in comparison to the frequency of laminin nanofibers without NGF. Neal *et al.* postulated that the topography and the associated high surface area of electrospun fibers were attributable to the extensions [43].

Layer-by-layer depositions, multilayer mixing, dual-mandrel electrospinning and magnetic electrospinning have also been used to manufacture multidimensional scaffolds [44-47]. Elastomeric vascular graft-fabrication methods have been investigated for over 30 years. Recent efforts have incorporated electrospinning to create a composite graft from poly(ethylene

oxide), segmented polyurethane and UV-crosslinked collagen I by rotating a traversing movable mandrel [44]. The use of cytotoxic crosslinkers was avoided for the bioadhesive, collagen component of the scaffold. Instead, UV crosslinking was used to render the collagen insoluble, but still capable of swelling.

Since the time that Kidoaki *et al*. demonstrated multidimensional construction of an electrospun vascular graft [44], other groups have proceeded to implant and characterize 3D electrospun scaffolds *in vivo*. Using sheep and rabbit models [48], a poly(ε-caprolactone) / collagen vascular graft was evaluated based upon functional and physiologic parameters such as patency, platelet adhesion resistance, as based on previous studies that had established upper limits for burst pressure (4912 ± 155 mmHg), tensile strength (4.0 ± 0.4 MPa) and adequate elasticity (2.7 ± 1.2 MPa) [49].

The current challenge is to devise methods that allow for reducing the cytotoxic solvent and / or crosslinker levels currently used to produce natural and natural / synthetic blended fibers [50]. The process of electrospinning often includes the addition of organic solvents to dissolve polymers prior to spinning [51]. Crosslinkers are used to strengthen spun fibers and render natural fibers more water resistant [42]. Some natural-spun fibers have circumscribed or reduced cytotoxic solvent or crosslinker usage by using techniques such as melt electrospinning, or by replacing organic solvents and crosslinkers with less toxic alternatives [40,43,52,53].

Electrospun fibers are increasingly becoming incorporated into many different applications. 3D tissues are being formed with spun nanofibers incorporated into composite designs [48,54-57], and hydrogel 3D composites with stitched fibers have been tested in animal models [54,55]. Thus, as biomimetic studies reduce the amount of cytotoxic crosslinkers and solvents used in electrospun scaffolds, continued efforts to improve biocompatibility may increase the frequency and efficacy of electrospun scaffold use in clinical trials for whole-organ engineering applications.

1.2.3. Responsive materials, remodeling and engineered gradients

The term ‘smart material’ encompasses many materials that recapitulate the dynamic nature of ECM remodeling in an engineered whole organ. Traditionally, ‘smart materials’ include materials such as piezoelectric sensors, shape memory alloys and polymer-responsive gels, which can respond to environmental fluctuations through physical or chemical changes. Smart polymers respond to changes in pH, ionic strength, chemical species, enzyme–substrate interactions, magnetic fields, temperature, electric fields, mechanical stimulation, as well as ultrasound irradiation [58,59]. These materials exploit responsiveness for a triggered release. In response to the changing environment, smart polymer hydrogels can swell, thus facilitating an intended deployment of the triggered response, such as drug release.

Various corneal tissue-engineering groups have harvested *ex vivo* cellular sources found in short supply, and expanded and implanted the cells using tissue sheet technologies that employ thermoreversible polymer coated tissue culture plates [60,62]. While poly(*N*-isopropylacrylamide) (PIPAAm) derived implanted cell sheets restored function to the affected corneas, PIPAAm derived cell sheets have most successfully been used in 2D applications to date, and cannot fully replicate cell-matrix remodeling dynamics of large, 3D organs [58]. The combined use of PIPAAm derived cell sheets with other synthetic scaffold materials and natural ECM polymers may be more successful in recapitulating 3D tissue and organ activities.

Natural matrix remodeling has been well documented in organs such as bone. In orthopedics, guided bone regeneration has been pursued using natural materials fabricated into scaffolds, such as demineralized bone, which possesses osteoinductive properties [62]. Recently, demineralized bone has been manufactured as a nanoscale bone matrix (NBM) powder and incorporated within poly(L-lactide) (PLA) electrospun fibers [63]. Human mesenchymal stem cells (MSCs) osteodifferentiated on both PLA and PLA-NBM scaffolds *in vitro*, and accelerated mineralization was observed of human MSC seeded PLA-NBM fibers implanted *in vivo* [64]. PLA-NBM also provided a scaffold exhibiting mechanical properties higher in average tensile strength and Young's modulus than PLA alone, while exhibiting lower values than cortical bone [63]. As a result, PLA-NBM constructs can provide osteoinductive cues and may approximate the mechanical properties of immature bone undergoing remodeling with minimal loading [63]. After 12 weeks *in vivo*, the defect was almost 90 % smaller than its original size, demonstrating the responsive remodeling potential of PLA-NBM [64].

Smart materials are seen as an attractive alternative to decellularized donor tissue, whose supplies will always remain limited. These smart materials preferably contain ECM molecules as well. To address this problem, Shiloh *et al.* developed a method to collect ECM secreted by skeletal muscle myoblasts, and form it into implantable smart scaffolds [65]. In this study, rat skeletal myoblasts were seeded onto foams that served as a scaffold. After 4 weeks in culture, a construction of skeletal myoblasts, ECM and scaffold material was formed. At this time, the scaffold was dissolved using a solvent; leaving behind tissue consisting of accumulated ECM and skeletal myoblasts. After decellularization the ECM was implanted in a rat dorsal subcutaneous site. At 4 weeks post-implantation, the implanted ECM materials were found to be incorporated into the surrounding tissue, and host cells had penetrated the material. By 12 weeks post-implantation almost all of the implanted ECM material was degraded.

Likewise, the fabrication of heart muscle using natural ECM matrices is being claimed as a new type of natural smart material [66]. Blan *et al*. manufactured a composite scaffold of chitosan, a natural biomaterial that was solubilized

with acetic acid, and later pH neutralized after freezing and lyophilization. Fibrinogen was added for scaffold gelation, followed by a thrombin coating, the incorporation of cardio myocytes and an added layer of fibrin. In terms of organ function, this group monitored contractility as well as ECM architecture. To create a responsive scaffold, degradation time was manipulated based upon lysozyme concentrations from 2 h – 2 weeks. One advantage of using a responsive enzyme-substrate scaffold is the ability to match changes in matrix metalloprotease activity to that of cell-secreted matrix remodeling [66,67]. With controlled degradation, cell migration can also be manipulated, although it is important to consider and control for potential unbalanced remodeling and tumorigenic consequences [68-70].

Scaffold degradation processes can also dynamically change cellular cues such as migration. As proteolytic activity degrades the ECM, cryptic binding sites are unveiled, and matrix-bound growth factors become untethered [68,71]. Cell migration occurring along a gradient, such as that which occurs during chemotaxis (chemical gradient), haptotaxis (cellular adhesion site gradients) and durotaxis (rigidity gradients), can therefore be manipulated based upon the design of the ECM [39,72]. Further studies in 3D have been able to demonstrate more physiologically relevant applications by creating matrices with natural materials that take advantage of durotaxis [73,74].

Although advances in whole-organ engineering have origins in 2D *in vitro* models, current methods for bioengineering functional tissues, including tissue decellularization and use of electrospun nanofibers and smart materials, are progressing to 3D scaffolds. It has been shown to be an oversimplification that cells behave the same in 3D as they behave in 2D [74-78]. Cell-matrix adhesions to the ECM are exaggerated in 2D cell cultures–the adhesions are stronger than those of cells in 3D models and of the cell *in vivo* [76]. Likewise, 3D matrix adhesions are not recreated in 2D [76]. Although better than 2D modeling, 3D models mimic static, short-term conditions and may oversimplify parameters such as oxygen diffusion [75,79]. Therefore, it is important and necessary to verify *in vitro* results with parallel *in vivo* model investigations.

1.3. WHOLE-TOOTH ENGINEERING

The tooth is an excellent example of a developing organ directed by the reciprocal interactions of mesenchymal and epithelial tissues over time [80]. Bioengineering strategies have targeted tooth regeneration using various combinations of scaffolds, growth factors and cells [81-84]. Approaches using tissue recombinations, and pelleting cells in a scaffold-free environment, are also popular strategies for whole-tooth engineering [85,86]. In addition, groups have investigated the location of the implantation site for engineered implants as a morphogenetic means of developmental signaling. The diastema, or toothless region within the rodent jaw, has been shown to provide a site for

whole-tooth formation, thus demonstrating the potential for teeth to regenerate and erupt in a native environment [87,88].

While cell pellets alone have been used in other studies to avoid the need for scaffolds [89,90], Nakao *et al.* included a collagen droplet method to contain pelleted E14.5 dental epithelial and mesenchymal cells within a collagen gel matrix [82]. Dissociated cell pellets generated from mouse embryonic molar and incisor dental epithelium and mesenchyme were both able to form predentin, dentin and enamel-like tissue, with specificity confirmed by *in situ* hybridization studies. These E14.5 droplet constructs were able to reassemble into proper tissue layers, whereas older E16.5 cells could not self assemble [82]. As the effects of collagen were not explored in this model, additional studies can be used to improve our understanding of ECM provided spatial and temporal cues for tooth development.

Ongoing studies in the Yelick laboratory have worked towards engineering a whole tooth, as well as hybrid tooth–bone constructs [91-97]. Notably, these studies have focused exclusively on the use of post-natal dental epithelial and mesenchymal tissue derived cells, as opposed to embryonic dental cells. Tooth regeneration studies using adult post-natal dental cells derived from unerupted pig molar teeth and human wisdom teeth are more relevant to human tooth tissue engineering, as human embryonic dental cell populations are generally not available for this purpose. In order for these approaches to achieve clinical status, what remains to be understood and perfected is how best to maintain the spatial organization of the dental epithelial and dental mesenchymal tissues, to guide not only the shape and size of a tooth and surrounding alveolar bone, but also to achieve proper compartmentalization of individual tissue types [92]. For instance, studies have observed ectopic alveolar bone growth within dental tissues [81,96]. Likewise, the ECM components associated with functional tooth-root formation and for functional tooth eruption are critical to our understanding. Histological and immunohistochemical approaches are followed to study the presence of critical ECM components like collagen, fibronectin, and laminin in bioengineered tooth-buds (Figure 1). Similarly, preliminary analyses in a 5.5 month old porcine molar model have demonstrated some ECM fiber organization within the bioengineered tooth-bud and surrounding alveolar bone. Areas of collagen, keratin and fibronectin were shown to co-localize within vascular regions of the dental pulp as well as in enamel epithelium [98]. Future studies will elucidate further ECM organization and composition in these bioengineered teeth.

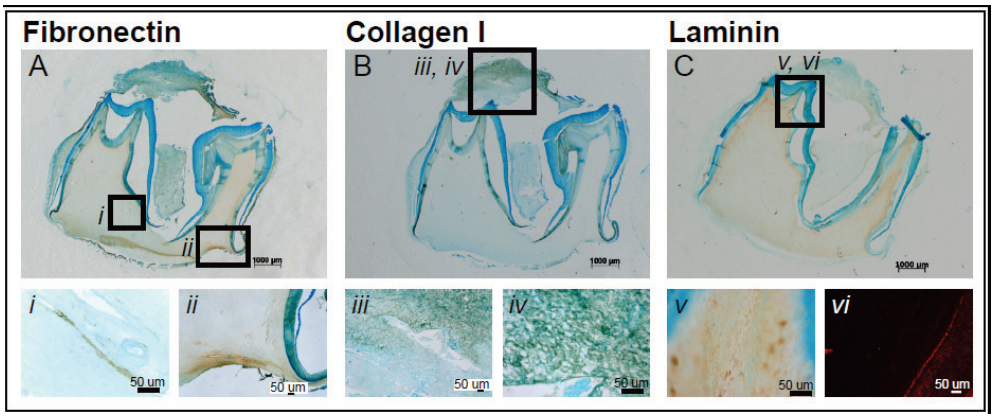

Figure 1. Immunohistochemical analyses of the extracellular organization of bioengineered porcine molar tooth-buds show positive staining for fibronectin (A), collagen I (B) and laminin (C). Higher magnification images of the boxes in (A) are found in (i) and (ii). Likewise, higher magnification images of the boxes in (B) and (C) are found in (iii), (iv) and (v). Fibronectin expression is observed in blood vessels and near odontoblasts (dental papilla). Collagen I is seen in the dental follicle, dentin and near odontoblasts. Laminin-α1 was stained brown in the dental papilla, follicle and dentin. Scale bars = 1000 µm in (A, B and C) and 100 µm in (i-vi).

With respect to human tooth re-engineering efforts, further characterization of the ECM molecules involved during critical stages of tooth development are imperative. Others have applied the roles of biglycan, and subsequent amelogenin expression, to nanofiber scaffolding to study enamel maturation [99-101]. Mouse knockout models have also elucidated the role of Tbx1 and enamel formation [102]. Still, further exploration of additional ECM molecules and corresponding spatial organization within the tooth are needed for the educated design of effective scaffolds for whole tooth tissue engineering. ECM molecules such as collagen I, osteocalcin, amelogenin, dentin matrix protein, dentin sialoprotein and bone sialoprotein were present in the bioengineered toothbud and tooth–bone hybrid constructs made of silk and poly(glycolic acid) (PGA) / poly(lactide-*co*-glycolide) (PLGA), respectively [92,95,96]. Some of these ECM molecules, such as collagen I, fibronectin, collagen IV, and laminin can be preserved in decellularized porcine tooth buds [103]. When reseeded with dental progenitor cells, these ECM molecules could contribute to an enhanced organization of the seeded cells. As we continue to characterize the locations and 3D organizations of additional fibrillar proteins and proteoglycans in native tissue and natural ECM scaffolds, we will gain an improved understanding of the spatial organization and function of the natural tissues within the tooth and bone, which guide and maintain final form and functions.

1.3.1. Ongoing challenges in whole-organ engineering

Thus far, the majority of clinically relevant grafts that have been constructed to date are designed for use in hollow organ regeneration and repair [55]. Implicit in the creation of solid organs, including teeth, is the proper integration of functional angiogenesis, lymphangiogenesis and neurogenesis within an organ or organ system [104,105]. An ongoing obstacle in angiogenesis is defining a targeted approach to facilitate invasion of vasculature into the developing organ, to provide sufficient oxygen to tissues with volumes greater than 2–3 mm^3. As host-vessel ingrowth requires a finite time to penetrate into the depth of the implanted tissue, necrosis can occur prior to sufficient vascularization, resulting in implant failure. Many studies have explored means to facilitate bioengineered angiogenesis [106,107] and ongoing *in vitro* attempts to prevascularize engineered tissue may have a future in *in vivo* applications [104,108-110]. Notably, one study has already demonstrated evidence of angiogenesis *in vivo* attributed to multi-cell type co-culture [111]. Others have incorporated mesenchymal cells with endothelial cells in 3D scaffold models to successfully create neo-vasculature network formation [112].

Despite these advances, the extent of successful penetration of functional host vessels into bioengineered tissues and organs has yet to be determined. Additional efforts have considered designing vascular network-based physiological models that consider length, diameter, pressure and flow rate, as vessels anastomose into vascular beds as well as recon-verge. These networks are especially applicable in branched, ordered tissues such as the lung or liver [105]. Furthermore, control of vessel architecture is relevant not only in terms of geometric function, but also in terms of maintaining vessel growth [70,105,113,114]. Specific to matrix-induced angiogenic efforts, groups are beginning to identify pro- and anti-angiogenic motifs on natural ECM peptides such as collagen IV [113,115,116]. From these data, gradients to drive angiogenic potential within a construct have been manufactured [117].

Another relatively new subset of angiogenic tissue engineering involves integrating lymphatic system formation in bioengineered tissues and organs. Similar concerns that exist in promoting angiogenesis persist with lymphatogenesis, in terms of controlling tissue growth and preventing metastatic behavior [118,119]. Animal models are currently being explored to investigate balancing pathologies in the lymphatic system [120-122]. However, it was found that lymphatic endothelial cells do not sprout to form a vessel unit, but rather the cells migrate to a site individually and allow unidirectional flow [123]. Perlecan, an ECM molecule involved in vascular homeostasis, was produced in a tissue-engineered model of skin regeneration within a rat model, although interestingly the ECM molecule was only formed after the construction of the lymph vessel and was expressed in the direction of flow [123]. Therefore, integration of a lymphatic system to prevent edema from

developing in an engineered organ may also be affected by changes in the ECM environment. As engineered organs become more prevalent, systemic integration with the lymphatic system will provide an immune response 'watchdog' to maintain homeostasis *via* lymphatic vessels, and to sustain hydrostatic and osmotic pressures at vessel-tissue interfaces [122].

Although tissue-engineering platforms exist to guide axonal growth [124], more cohesive strategies are needed to innervate engineered constructs in a controlled manner. Currently, autologous epineurium [125], or better still an autologous sural graft [126], serve as gold standards for peripheral nerve regeneration. However, autografts have caveats, from supply shortages to the fact that they may not be made-to-order in terms of nerve length, may create wound pain and often have a motor function recovery rate of less than 40 % [125,126]. To innervate an organ, the graft should match the mechanical properties of surrounding areas, allow for diffusion, provide the appropriate degradation when a nerve regenerates and provide migratory guidance cues to recruit nearby axons from a neural growth cone or other means of taxis [124,126]. Current neural-tube materials include, but are not limited to, PGA–collagen, PLGA, poly(L-lactic acid), silicon and hydroxyapatite (HA)-collagen hydrogels [125,126]. While synthetic neural tubes may offer improved stiffness, the same synthetic materials have caused complications such as inflammatory responses and scarring [125,126].

Directing neurogenesis in a precise manner for efficient integration of implanted tissues within the host, and to test for restored function of the nerve, are ongoing struggles. A recent rabbit facial nerve defect model, which tested a HA-collagen hydrogel construct with NT-3 growth factor and xenogenic neural stem cells, found minimal signs of immune response and successful migration of donor cells to affected areas [125]. However, Zhang *et al.* were not able to demonstrate improved neuromuscular function using HA-collagen implants, based on ethology and electromyography results. Functional innervation studies are still difficult to prove in animal models, although various tests have been established for peripheral nerve recovery [126,127]. As Li *et al.* have previously surmised that axonal guidance needs multiple cues for nerve regeneration, which could include integrating physical stimulation [124]. For example, 780 nm laser phototherapy, when applied transcutaneously to peripheral nerve-damaged patients, significantly improved motor function as well as voluntary muscle activity in partially paralyzed limbs [128]. These studies demonstrate that cell growth and specific antibody expression should be coupled to a test of restored function, and may need to include multiple cues for guided regeneration.

1.4. UNMET NEEDS

Efforts to engineer organs, including teeth, are still struggling to identify available and reliable cell sources, and to optimize efficient incorporation of cells into scaffolds. While the multipotency of adult stem cells is being realized as an autologous source for various tissues, limitations remain for re-engineering immature tissue [129]. For instance, since enamel forming tissues have undergone apoptosis prior to tooth eruption, it is necessary to identify a dental epithelial cell source for bioengineered enamel production. Although current studies use murine, rat and porcine tooth germ tissues, animal-derived cells are not suitable for clinical applications in humans. Epithelial Rests of Malassez (REM), present in mature human periodontal tissues, may be a suitable source for human dental epithelium [130]. In addition, current attempts to reprogram cell sources include the development of spontaneously derived immortalized murine dental epithelial cell lines, which when grown in low calcium-supplemented media, can express enamel markers such as amelogenin [131,132], and the use of single-cell suspensions generated from tooth germ tissue [133]. Lessons from these studies should assist efforts to generate suitable human dental epithelial cell lines from available tissues such as Hertwig's epithelial root sheath or epithelial cell REM. Recently, however, Sharpe *et al.* used adult human gingival cells as an epithelial cell source. When combined with mouse embryonic tooth-inducing mesenchyme cells, dental tissue was formed. The adult human gingival cells contributed to the formation of ameloblast-like cells and rests of Malassez [134]. Furthermore, chimeric teeth, generated from autologous dental mesenchyme combined with xenogenic dental epithelium, may eventually be used as a clinically relevant alternative approach [86,90].

Incorporating cells into decellularized and / or fabricated scaffolds is also a parameter in need of improvement. While many studies use bioreactors to facilitate cell seeding, reports of uneven adhesion and proliferation persist [11,32]. Direct injection of cells into scaffolds may create cell clusters rather than even cell distributions, depending on cell migration and cell adhesion receptor binding sites. For example, although Blan *et al.* directly injected cardiomyocytes into smart chitosan material, this approach did not produce the necessary contractile responses owing to low cell retention. However, injection of cells mixed with fibrin gel allowed for cell adhesion to the scaffold [66]. Methods for cell penetration into, retention on and proliferation within scaffolds are anticipated to improve as strategies to promote angiogenesis throughout bioengineered organs continue to advance, and allow for continuous recruitment of host progenitor cells to the implant site. As supporting scaffolds degrade over time, questions remain, such as: Will the regenerating tissue unit be able to grow and remodel? Will engineered organs possess the appropriate ECM signals for proper growth and remodeling, based upon the proposed regression, and pruning models of blood vessel and nerve formation [71,113,126]? Although defined methods to properly manipulate

and monitor angiogenesis, lymphangiogenesis and neurogenesis in bioengineered organs remain unclear, they will undoubtedly improve as additional functional, long-term studies using whole-engineered organs are completed.

1.5. FUTURE PERSPECTIVE

Whole-organ engineering is a new field with plenty of room to grow, and a multitude of multi and inter-disciplinary talents are involved in this pursuit. As we continue to learn more about natural ECM materials, fabrication technologies will also advance. Over the next few years, we will continue to learn more about the composition, degradation and remodeling rates of decellularized cadaveric allografts, as the demand for clinical studies and the number of potential commercial products increases, and as methods for improved removal and detection of MHC antigens continue to improve. As microarray techniques continue to improve high throughput screening, we will be able to better characterize serology screens for foreign antigens in decellularized cadaveric tissues.

Likewise, the generation of thin electrospun fibers with less toxic solvents and crosslinkers will improve current tissue-engineering efforts. Natural crosslinkers, such as genipin, have already shown improved biocompatibility over glutaraldehyde in tissue fixation [135-137]. Other groups have demonstrated incorporation of genipin into natural ECM hydrogels [73,138] and natural electrospun nanofibers [53]. With improved nanofiber production methods, more complex 3D electrospinning techniques can be used to find better ways to integrate a variety of fabricated scaffold layers on the mesoscopic scale.

Smart polymer technologies should increase in clinical relevance as the demonstrated use of composite corneal implants becomes more prevalent. As 3D synthetic scaffolds develop or as natural ECM analogs are better characterized based on remodeling characteristics, implants will become more dynamic, thus reducing the number of surgeries needed for a procedure. Similarly, more long-term studies will assist in our understanding of the biocompatibility and degradation processes of scaffolds over time, along with the associated cascade of matrix metalloprotease activities and soluble cytokines, which redefine and remodel the ECM. Looking beyond the next few years, pluripotent reprogramming technologies such as induced pluripotent stem cells and piggyBac will continue to improve [139-141], and new and useful human embryonic cell lines will be created. Thus, these cells will provide new sources for organ engineering to study ECM synthesis and turnover. As instructive scaffold technologies continue to improve, we anticipate being able to directly control and monitor cell behavior, migration and differentiation throughout the morphogenetic process of any organ

formation. As such, the field of whole-organ tissue engineering has a bright and promising future.

REFERENCES

1. Y.L. Cao, J.P Vacanti, *39th Annual Meeting of the Plastic Surgery Research Council,* Transplantation of chondrocytesutilizing a polymer–cell construct to produce tissue-engineered cartilage in the shape of a humanear, Ann Arbor, MI, USA. 1994.
2. S.J. Shieh, S. Terada. *Biomaterials* **25** (2004) 1545–1557.
3. B.O. Palsson, S.N. Bhatia, *Tissue Engineering*, Pearson Prentice Hall, NJ, USA, 2004, p. 20–33.
4. J.F. Mano, G.A Silva. *J. R. Soc. Interface* **4** (2007) 999–1030.
5. I. Capila, R.J. Linhardt. *Angew. Chem. Int. Ed.* **41** (2002) 391–412.
6. J.H. Miner, P.D. Yurchenco. *Ann. Rev. Cell Dev. Biol*. **20**(2004) 255–284.
7. J.H. Miner. *Microsc. Res. Tech.* **71** (2008) 349–356.
8. M. van der Rest, R. Garrone. *FASEB J*. **5** (1991) 2814–2823.
9. F. Bolland, S. Korossis. *Biomaterials* **28** (2007) 1061–1070.
10. S.F. Badylak. *Transpl. Immunol.* **12** (2004) 367–377.
11. A. Ketchedjian, A.L. Jones. *Ann. Thorac. Surg.* **79** (2005) 888–896.
12. K. Schenke-Layland, O. Vasilevski. *J. Struct. Biol*. **143** (2003) 201–208.
13. I. Tudorache, S. Cebotari. *J. Heart Valve Dis.* **16** (2007) 567–573.
14. M.T. Kasimir, E. Rieder. *J. Heart Valve Dis.* **15** (2006) 278–286.
15. E. Rieder, M.T. Kasimir. *J. Thorac. Cardiovasc. Surg.* **127** (2004) 399–405.
16. R.L. Knight, H.E. Wilcox. *Proc. Inst. Mech. Eng. H* **222** (2008) 129–143.
17. J. Liao, E.M. Joyce. *Biomaterials* **29** (2008) 1065–1074.
18. S. Mirsadraee, H.E. Wilcox. *Tissue Eng.* **12** (2006) 763–773.
19. M.T. Conconi, P. De Coppi. *Transpl. Int.* **18** (2005) 727–734.
20. P. Macchiarini, P. Jungebluth. *Lancet* **372** (2008) 2023–2030.
21. A.D. Bhrany, B.L. Beckstead. *Tissue Eng.* **12** (2006) 319–330.
22. S.B Lumpkins, N. Pierre. *Acta Biomater.* **4** (2008) 808–816.
23. S.F. Badylak. *Biomaterials* **28** (2007) 3587–3593.
24. T.W. Gilbert, T.L. Sellaro. *Biomaterials* **27** (2006) 3675–3683.
25. W. Konertz, P.M. Dohmen. *J. Heart Valve Dis* **14** (2005) 78–81.
26. C. Harper, *Hosp. Med* **62** (2001) 90–95.
27. P.M. Dohmen, S. Hauptrnann. *J. Heart Valve Dis.* **16** (2007) 447–449.
28. S.P. Marquez, V.S. Martinez. *Acta Biomater*. **5** (2009) 1839–1847.
29. E. Rieder, A. Nigisch. *Biomaterials* **27** (2006) 5634–5642.
30. T.W. Stapleton, J. Ingram. *Tissue Eng. Part A* **14** (2008) 505–518.
31. R.D. Harrison, P.F. Gratzer. *J. Biomed. Mater. Res. A* **75A** (2005) 841–854.
32. H.C. Ott, T.S. Matthiesen. *Nat. Med.* **14** (2008) 213–221.
33. N.E. Bühler, K. Schulze-Osthoff. *J. Biosci. Bioeng.* **119** (2015) 609–613.
34. A.P. Price, L.M. Godin. *Tissue Eng. Part C Methods* **21** (2015) 94–103.
35. P.F. Gratzer, R.D. Harrison. *Tissue Eng.* **12** (2006) 2975–2983.
36. J.H. Ingram, S. Korossis. *Tissue Eng.* **13** (2007) 1561–1572.
37. E.K. Merritt, M.V. Cannon. *Tissue Eng. Part A* **16** (2010) 2871–2881.
38. P.A. Jimenez, S.E Jimenez. *Am. J. Surg.* **187** (2004) S56–S64.
39. J.E. Reing, L. Zhang. *Tissue Eng. Part A* **15** (2009) 605–614.

40. S. Agarwal, J.H. Wendorff. *Polymer* **49** (2008) 5603–5621.
41. J. Yuan, J. Shen. *Polym. Int.* **57** (2008) 1188–1193.
42. T.G. Kim, H.J. Chung. *Acta Biomater*. **4** (2008) 1611–1619.
43. R.A. Neal, S.G. McClugage. *Tissue Eng. Part C* **15** (2009) 11–22.
44. S. Kidoaki, I.K. Kwon. *Biomaterials* **26** (2005) 37–46.
45. K. Klinkhammer, N. Seiler. *Tissue Eng. Part C Methods* **15** (2009) 77–85.
46. P.D. Dalton, D. Klee. *Polymer* **46** (2005) 611–614.
47. D. Yang, B. Lu. *Adv. Mater.* **19** (2007) 3702–3706.
48. B.W. Tillman, S.K. Yazdani. *Biomaterials* **30** (2009) 583–588.
49. S.J. Lee, J. Liu. *Biomaterials* **29** (2008) 2891–2898.
50. J.W. Xie, X.R. Li. *Macromol. Rapid Commun.* **29** (2008) 1775–1792.
51. Z.M. Huang, Y.Z. Zhang. *Polymer* **45** (2004) 5361–5368.
52. H.C. Chen, W.C. Jao. *Polym. Adv. Technol*. **20** (2009) 98–103.
53. S.S. Silva, D. Maniglio. *Macromol. Biosci*. **8** (2008) 766–774.
54. X. Chen, Y.Y. Qi. *Biomaterials* **29** (2008) 3683–3692.
55. D. Eberli, L.F. Filho. *Methods* **47** (2009) 109–115.
56. A.K. Ekaputra, G.D. Prestwich. *Biomacromolecules* **9** (2008) 2097–2103.
57. L. Moroni, R. Schotel. *Adv. Mater.* **18** (2008) 53–60.
58. P.M. Mendes. *Chem. Soc. Rev.* **37** (2008) 2512–2529.
59. J.F. Mano. *Adv. Eng. Mater.* **10** (2008) 515–527.
60. T. Sumide, K. Nishida. *FASEB J.* **20** (2006) 392–394.
61. G. Sitalakshmi, B. Sudha. *Tissue Eng. Part A* **15** (2009) 407–415.
62. J.R. Lieberman, G.E. Friedlaender. *Bone Regeneration and Repair: Biology and Clinical Applications*, Humana Press, NY, USA, 2005.
63. E.K. Ko, S.I. Jeong. *Macromol. Biosci.* **8** (2008) 1098–1107.
64. E.K. Ko, S.I. Jeong. *Tissue Eng. Part A* **14** (2008) 2105–2119.
65. S.A. Hurd, N.M. Bhatti. *Biomaterials* **49** (2015) 9–17.
66. N.R. Blan, R.K Birla. *J. Biomed. Mater. Res. A* **86A** (2008) 195–208.
67. A.M. Martins, M.I. Santos. *Acta Biomater.* **4** (2008) 1637–1645.
68. W.P. Daley, S.B. Peters. *J. Cell Sci.* **121** (2008) 255–264.
69. V. Nikolova, C.Y. Koo. *Carcinogenesis* **30** (2009) 397–407.
70. C. Chang, Z. Werb. *Trends Cell Biol.* **11** (2001) S37–S43.
71. C.M. Ghajar, S.C. George. *Crit. Rev. Eukaryot. Gene Expr.* **18** (2008) 251–278.
72. M.E. Fleury, K.C. Boardman. *Biophys. J.* **91** (2006) 113–121.
73. H.G. Sundararaghavan, G.A. Monteiro. *Biotechnol. Bioeng.* **102** (2009) 632–643.
74. E. Hadjipanayi, V. Mudera. *Cell Motil. Cytoskeleton* **66** (2009) 121–128.
75. K.M. Yamada, E. Cukierman. *Cell* **130** (2007) 601–610.
76. E. Cukierman, R. Pankov. *Science* **294** (2001) 1708–1712.
77. M. Singh, C. Berkland. *Tissue Eng. Part B Rev.* **14** (2008) 341–366.
78. F. Pampaloni, E.G. Reynaud. *Nat. Rev. Mol. Cell Biol.* **8** (2007) 839–845.
79. C.M. Ghajar, X. Chen. *Biophys. J.* **94** (2008) 1930–1941.
80. I. Thesleff, A.M. Partanen. *J. Craniofac. Genet. Dev. Biol.* **11** (1991) 229–237.
81. Y.C. Li, F. Jin. *Tissue Eng. Part A* **14** (2008) 1731–1742.
82. K. Nakao, R. Morita. *Nat. Methods* **4** (2007) 227–230.
83. E.L. Scheller, P.H. Krebsbach. *J. Oral Rehabil.* **36** (2009) 368–389.
84. M.J. Honda, H. Fong. *Med. Mol. Morphol.* **41** (2008)183–192.
85. B. Hu, A. Nadiri, *8th International Conference on Tooth Morphogenesis and Differentiation, Tissue engineering of tooth crown, root, and periodontium*, York, UK, 2004.

86. J.H. Yu, J.N. Shi. *Tissue Eng. Part B Rev.* **14** (2008) 307–319.
87. A. Ohazama, S.A.C Modino. *J. Dent. Res.* **83** (2004) 518–522.
88. Y.Q. Song, M.Q. Yan. *Dev. Dyn*. **237** (2008) 411–416.
89. J.H. Yu, J.N. Shi. *Biochem. Biophys. Res. Commun*. **346** (2006) 116–124.
90. C.F. Ferreira, R.S. Magini, *2nd Journal of Oral Rehabilitation Summer School, Biological tooth replacement and repair,* Bevagma, Italy, 2006.
91. S.E. Duailibi, M.T. Duailibi. *J. Dent. Res.* **87** (2008) 745–750.
92. W.P. Xu, W. Zhang. *Tissue Eng. Part A* **14** (2008) 549–557.
93. M.T. Duailibi, S.E. Duailibi. *J. Dent. Res.* **83** (2004) 523–528.
94. C.S. Young, S. Terada. *J. Dent. Res.* **81** (2002) 695–700.
95. C.S. Young, H. Abukawa. *Tissue Eng.* **11** (2005) 1599–1610.
96. W.B. Zhang, H. Abukawa. *Methods* **47** (2009) 122–128.
97. H. Abukawa, W. Zhang. *J. Oral Maxillofac. Surg.* **67** (2009) 335–347.
98. S.B. Traphagen, P.C. Yelick. *Regen. Med.* **4** (2009) 747–758.
99. X. Wen, Y.M. Zou. *Anat. Rec.* **291** (2008) 1246–1253.
100. D.M.H. Tenorio, M.F. Santos, *International Symposium on Extracellular Matrix (SIMEC 2002),* Distribution of biglycan and decorin in rat dental tissue, Angra dos Reis, RJ, Brazil. 2002.
101. Z. Huang, T.D. Sargeant. *J. Bone Miner. Res.* **23** (2008) 1995–2006.
102. J. Caton,H.U. Luder. *Dev. Biol.* **328** (2009) 493–505.
103. S.B. Traphagen, P.C. Yelick. *Biomaterials* **33** (2012) 5287–5296.
104. J.J. Moon, J.L. West. *Curr. Top. Med. Chem*. **8** (2008) 300–310.
105. D.M. Hoganson, H.I. Pryor. *Pediatr. Res.* **63** (2008) 520–526.
106. E.M. Brey, S. Uriel. *Tissue Eng*. **11** (2005) 567–584.
107. P. Carmeliet. *J. Intern. Med.* **255** (2004) 538–561.
108. C.K. Griffith, C. Miller. *Tissue Eng.* **11** (2005) 257–266.
109. N.C. Rivron, J. Liu. *Eur. Cell. Mater.* **15** (2008) 27–40.
110. M.I. Santos, K. Tuzlakoglu. *Biomaterials* **29** (2008) 4306–4313.
111. S. Levenberg, J. Rouwkema. *Nat. Biotechnol.* **23** (2005) 879–884.
112. N. Koike, D. Fukumura. *Nature* **428** (2004) 138–139.
113. G.E. Davis, D.R. Senger. *Circ. Res.* **97** (2005) 1093–1107.
114. S.E. Epstein, R. Kornowski. *Circulation* **104** (2001) 115–119.
115. J. Sottile. *Biochim. Biophys. Acta* **1654** (2004) 13–22.
116. E.D. Karagiannis, A.S. Popel. *Biochem. Biophys. Res. Commun.* **354** (2007) 434–439.
117. C. Borselli, O. Oliviero. *J. Biomed. Mater. Res. A* **80A** (2007) 297–305.
118. L.G. Griffith, M.A. Swartz. *Nat. Rev. Mol. Cell Biol.* **7** (2006) 211–224.
119. H.M.E. Hajjami, T.V. Petrova. *Histochem. Cell Biol.* **130** (2008) 1063–1078.
120. W.S. Shin, S.G. Rockson. *Ann. NY Acad. Sci.* **1131** (2008) 50–74.
121. S. Suematsu, T. Watanabe. *Nat. Biotechnol.* **22** (2004) 1539–1545.
122. M.A. Swartz, J.A Hubbell. *Semin. Immunol.* **20** (2008) 147–156.
123. J.M. Rutkowski, K.C. Boardman. *Am. J. Physiol. Heart Circ. Physiol.* **291** (2006) H1402–H1410.
124. G.N. Li, D. Hoffman-Kim. *Tissue Eng. Part B Rev.* **14** (2008) 33–51.
125. H. Zhang, Y.T. Weing. *J. Transl. Med.* **6** (2008) 67.
126. S. Ichihara, Y. Inada. *Injury* **39** (2008) S29–S39.
127. C.M. Nichols, T.M. Myckatyn. *Behav. Brain Res.* **163** (2005) 143–158.
128. S. Rochkind. *Neurosurg. Focus* **26** (2009) E8.
129. C. Morsczeck, G. Schmalz. *Clin. Oral Invest.* **12** (2008) 113–118.

130. H. Nam, J.H. Kim. *Mol. Cells* **37** (2014) 562–567.
131. A. Nakata, T. Kameda. *Biochem. Biophys. Res. Commun*. **308** (2003) 834–839.
132. A. Komine, M. Suenaga. *Biochem. Biophys. Res. Commun*. **355** (2007) 758–763.
133. S. Iwatsuki, M.J. Honda. *Eur. J. Oral Sci.* **114** (2006) 310–317.
134. A. Angelova Volponi, M. Kawasaki. *J. Dent. Res*. **92** (2013) 329–334.
135. A. Bigi, G. Cojazzi. *Biomaterials* **23** (2002) 4827–4832.
136. S.M. Lien, W.T. Li. Mater. *Sci. Eng. Biomim. Mater. Sens. Syst*. **28** (2008) 36–43.
137. W.H. Chang, Y. Chang. *J. Biomater. Sci. Polym. Ed* **14** (2003) 481–495.
138. H.G. Sundararaghavan, G.A. Monteiro. *J. Biomed. Mater. Res. A* **87A** (2008) 308–320.
139. K. Takahashi, S. Yamanaka. *Cell* **126** (2006) 663–676.
140. K. Kaji, K. Norrby. *Nature* **458**(7239) (2009) 771–775.
141. K. Woltjen, I.P Michael. *Nature* **458**(7239) (2009) 766–770.